

N71-12892

Plasma Dynamics Laboratory  
Technical Report 70-2

October 1970

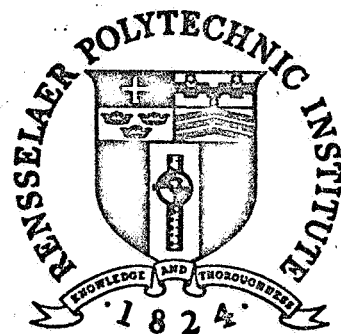
13 To  
clearing  
house

INSTABILITIES and TURBULENCE  
in HIGHLY IONIZED PLASMAS  
in a MAGNETIC FIELD

by J. H. NOON, G. HUCHITAL, W. C. JENNINGS

CASE FILE  
COPY

Semi Annual Status Report  
NASA Grant No. 33-018-137  
March 1, 1970-August 31, 1970



Electrophysics Division  
Rensselaer Polytechnic Institute  
Troy, New York

## SUMMARY

Correlation studies show that some degree of coherence exists throughout the whole of the observed plasma turbulence spectrum, although time and length scales of coherence decrease markedly with increasing frequency. Propagation characteristics and energy dissipation mechanisms of these turbulent eddies are being investigated. We find that growth of a strongly coherent drift wave instability is associated with an increase in amplitude of the high frequency end of the turbulence spectrum. On the other hand growth of another type of coherent oscillation (an ion acoustic wave) reduces the amplitude of the turbulent spectrum, but only in the frequency regions adjacent to that of the strong coherent oscillation. Further experimental data is required before these results can be related to theoretical work.

## I. Introduction

Turbulent fluctuations of electrostatic fields and charged particle density in a plasma medium are connected with plasma transport properties.<sup>13,18</sup> However the study of plasma turbulence is even more complex than the study of fluid turbulence, because charged particles give rise to collective oscillations in a plasma medium. Collective oscillations are rarely observed in a fluid.

By inserting a Langmuir probe in the plasma and displaying the resulting signal on a spectrum analyzer we observe the oscillations in plasma potential if the probe is at floating potential, or the oscillations in charged particle density if the probe is biased into the ion saturation region. All data presented in this report were obtained by use of probes at floating potential.

Our spectrum analyzer can be used to display the amplitude of the signal versus frequency for frequencies up to 1 MHz. The spectrum is continuous over this range, see Fig. 1-1. By varying some of the external parameters associated with the operation of the arc such as background pressure, gas flow through anode and cathode, magnetic field strength and magnetic field geometry, we can cause the onset of large amplitude coherent oscillations, see Fig. 1-2, and also affect the level of the turbulent oscillations. Although the rest of the oscillations are lower in amplitude, they occupy a larger portion of the spectrum than the coherent oscillation. We are, therefore, interested in the effect of the onset and growth of these instabilities on the complete spectrum of oscillations.

Calculation of an auto correlation function for specific oscillations leads to a power spectrum. By monitoring changes in the power spectrum associated with changing external plasma parameters we can establish the form of coupling between the large coherent instabilities and the turbulent portion of the spectrum. It has already been shown that anomalous plasma diffusion across the magnetic field is related to the presence of large coherent instabilities<sup>1,2,3,6,12</sup>, and the study of these coupling effects should give useful information about the energy exchange process involved in the plasma.

Using this correlation technique we were able to detect some degree of coherence for oscillations throughout the frequency spectrum up to 100 KHz, and also obtain order of magnitude estimates of the temporal extent of these oscillations. Calculation of cross correlation functions for different oscillations in the plasma was used to obtain propagation characteristics of these oscillations and the order of magnitude of the spatial extent of these fluctuations.

## II. Power Spectra

The recent acquisition of new instrumentation allowed us to measure power spectra<sup>4,14,15</sup>, that is, to plot power contained at each oscillation frequency of the plasma, in a more reliable way than can be done from a spectrum analyzer. The PAR Model 102 Fourier Analyzer gives the power spectrum directly from an auto correlation function of the fluctuations detected by a Langmuir probe. This instrument is designed to make use of the Weiner autocorrelation theorem, which states that the Fourier cosine transform

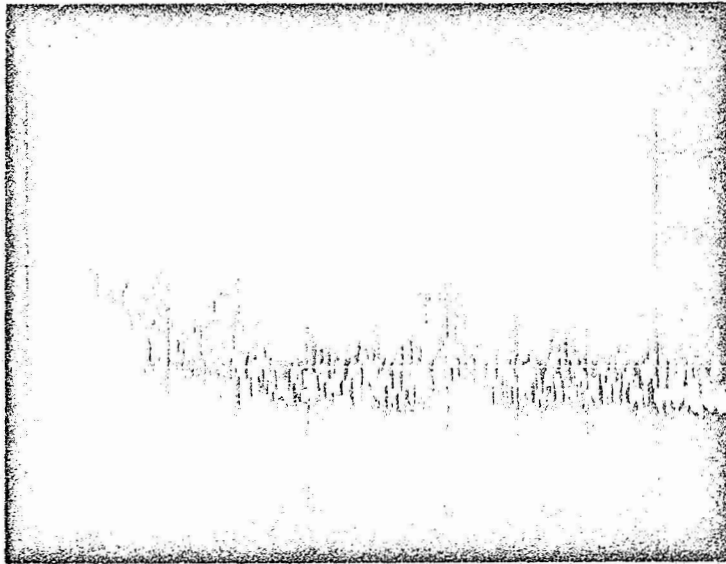


Figure 1-1 Spectrum Analyzer Frequency versus Amplitude, 10-1000 KHz,  
.01 V/cm

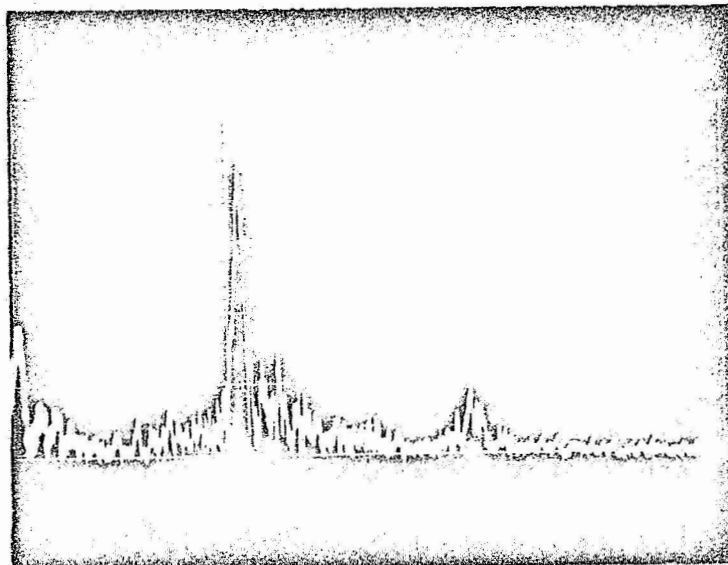


Figure 1-2 Spectrum Analyzer Frequency versus Amplitude, 0-10 KHz,  
.2 V/cm

of the auto correlation function  $C_{11}(\tau)$  gives directly the power spectrum of oscillations,  $\phi_{11}(\omega)$ :

$$\phi_{11}(\omega) = 2 \int_0^{\infty} C_{11}(\tau) \cos \omega \tau \, d\tau \quad 2-1$$

When external plasma parameters such as magnetic field, neutral gas pressure, and gas flow rates through both anode and cathode are varied, the observed power spectra exhibit definite changes. By establishing the connection between the characteristics of the turbulence spectra, the development of strong coherent oscillations, and the internal parameters of the arc, we can therefore investigate energy exchange mechanisms experimentally.

Theoretical work along these lines has been carried out, for example, by Tchen<sup>16,17</sup>. He has considered the spectral distribution of energy for charged-particle density fluctuations in a plasma in a strong magnetic field, for both the collisionless and the collision-dominated case. Describing the plasma by the Navier-Stokes equation of motion including an electrostatic field, the equation of continuity for a compressible fluid, and the Poisson equation for charge densities, he solved the resulting non-linear equation using an approximation called cascade decomposition. The Fourier components of all eddies were grouped into two separate parts: large-scale eddies, which contribute to the development of the energy spectra, and smaller eddies which set up turbulent properties. The turbulent motion of the big eddies was considered homogeneous, stationary, isotropic and compressible. The small eddies were assumed incompressible, non-homogeneous, anisotropic, non-stationary and did not contain as much energy as the large scale eddies.

Two different energy exchange mechanisms had to be assumed to account for the modal transfer from big eddies to smaller ones. Dissipation, or a drain of energy was assumed to occur for the collision dominated plasma by a molecular viscosity, and for the collisionless plasma, by collective electrostatic fluctuations. The spectra derived under these assumptions depend on the wave number  $k$  of the oscillations raised to an appropriate power.

For the collisional plasma the density fluctuation spectrum can be represented as

$$G \propto k^{-3/2} \quad k < k_B$$

or

$$G \propto k^{-9/2} \quad k > k_B$$

where  $k_B = (4 \alpha / a \lambda^2)^{1/2}$

$$\alpha = (\epsilon \omega_c / 2)^{1/2}$$

$\epsilon$  = a dissipation quantity

$\lambda$  = coefficient of Bohm diffusion

$\omega_c$  = cyclotron frequency

For the collisionless plasma the density fluctuation spectrum

$$G \propto k^{-5}$$

These expressions show how the type of energy dissipative mechanisms affect the shape of the spectrum of density fluctuations.

In order to experimentally test the results of Tchen's theory it is necessary to isolate various wave number components and find the power

present in each component. However techniques for the isolation of particular wave number components are not available at this time, and in the present experiment particular frequency intervals were isolated. Therefore a method of converting from a frequency to a wave number spectrum is needed in order to test theoretical expressions which have been derived. One possible technique for converting from frequencies to wave number ( $\omega \rightarrow k$ ) is proposed in a later section.

In our experiment three different operating regions of the plasma were selected and the effect of neutral gas pressure on the power spectrum was studied:

(i) a quiescent regime of the plasma with neutral gas pressure  $p = 1.9 \times 10^{-4}$  torr, main solenoid magnetic field  $B = 770$  gauss, and the magnetic field in the neighborhood of the cathode,  $B_c = 385$  gauss.

(ii) a regime where, by reducing the flow-rate of argon through the cathode 20%, onset and growth of one coherent instability, an ion acoustic wave, at about 4 KHz in the frequency spectrum was initiated.

(iii) a regime where the onset and growth of another type of coherent instability, a drift wave, at about 7 KHz in the frequency spectrum was initiated. This was accomplished by increasing  $B$  to 2100 gauss and adjusting  $B_c$  to the same value.

The effect of pressure change in region (i) is shown in Fig. 2-1. The neutral gas pressure was increased from an initial value of  $1.9 \times 10^{-4}$  torr, first 20%, and then 60%, by closing the baffles between the system and the diffusion pumps. The following changes in the power spectrum are observed: at the low frequency end, magnitudes are affected by up to 100% but there



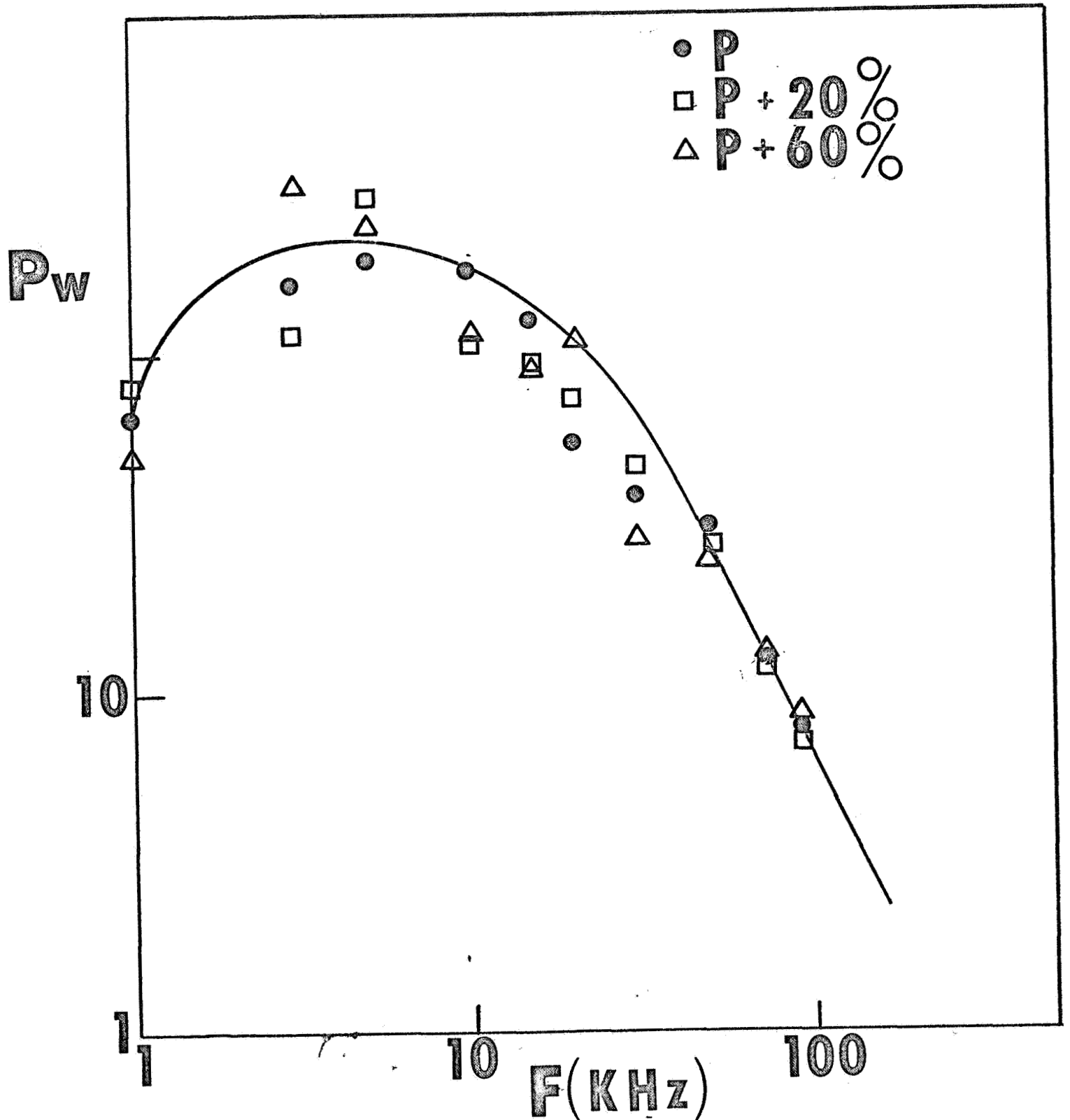


Figure 2-1 Power Versus Frequency  
Power in arbitrary units - initial pressure  $P = 1.9 \times 10^{-4}$  torr.  
 $B_H = 770$  gauss,  $B_C = 385$  gauss

is no systematic change with increasing pressure. At the high frequency end the slope of the power spectrum is unchanged.

The effect of pressure change in regime (ii) is shown in Fig. 2-2. It should be noted that initially the power contained in the coherent oscillation at around 4 KHz is at least 60 times the power contained in adjacent frequency components of the turbulent spectrum. By increasing the pressure in the same way as before, the amplitude of the ion acoustic wave can be reduced to the point where the wave is no longer distinguishable from those oscillations around it. The two power spectra (with and without the ion acoustic wave) are shown in Fig. 2-2 and it is clear that the power in the oscillations at frequencies on either side of the ion acoustic wave increases as the power in the coherent oscillation decreases. However the high frequency end of the spectrum is unaffected. This suggests that the ion acoustic wave gains some of its energy at the expense of those low frequency oscillations which surround it on the frequency spectrum.

The effect of pressure change in regime (iii) is shown in Fig. 2-3. In this case the strong oscillation at around 7 KHz is a drift wave, and the power contained in this oscillation is about 60 times the power contained in adjacent frequencies of the turbulent spectrum. It can be seen in Figure 2-3 that reducing the amplitude of this coherent instability by increasing the pressure by 60% has little effect upon the low frequency end of the power spectrum. However there is a noticeable change in the slope of the power spectrum above 50 KHz.

The slope of power spectra 2-1 through 2-3 are all different, which suggests that different energy exchange mechanisms are present when a

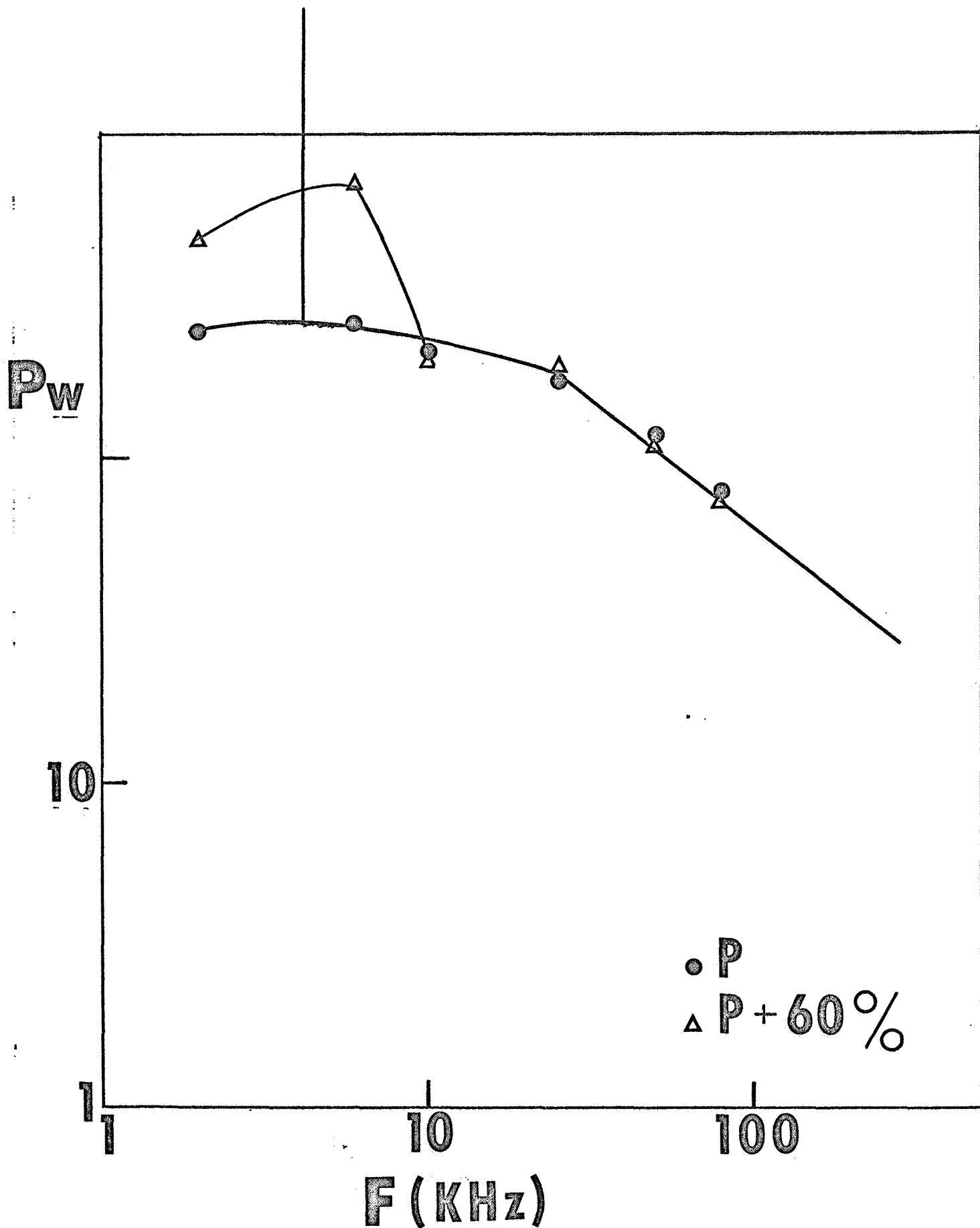


Figure 2-2 Power Versus Frequency. (ion acoustic wave) Power in arbitrary units - initial pressure  $P = 1.9 \times 10^{-4}$ ,  $B_H = 770$  gauss  $B_c = 385$  gauss

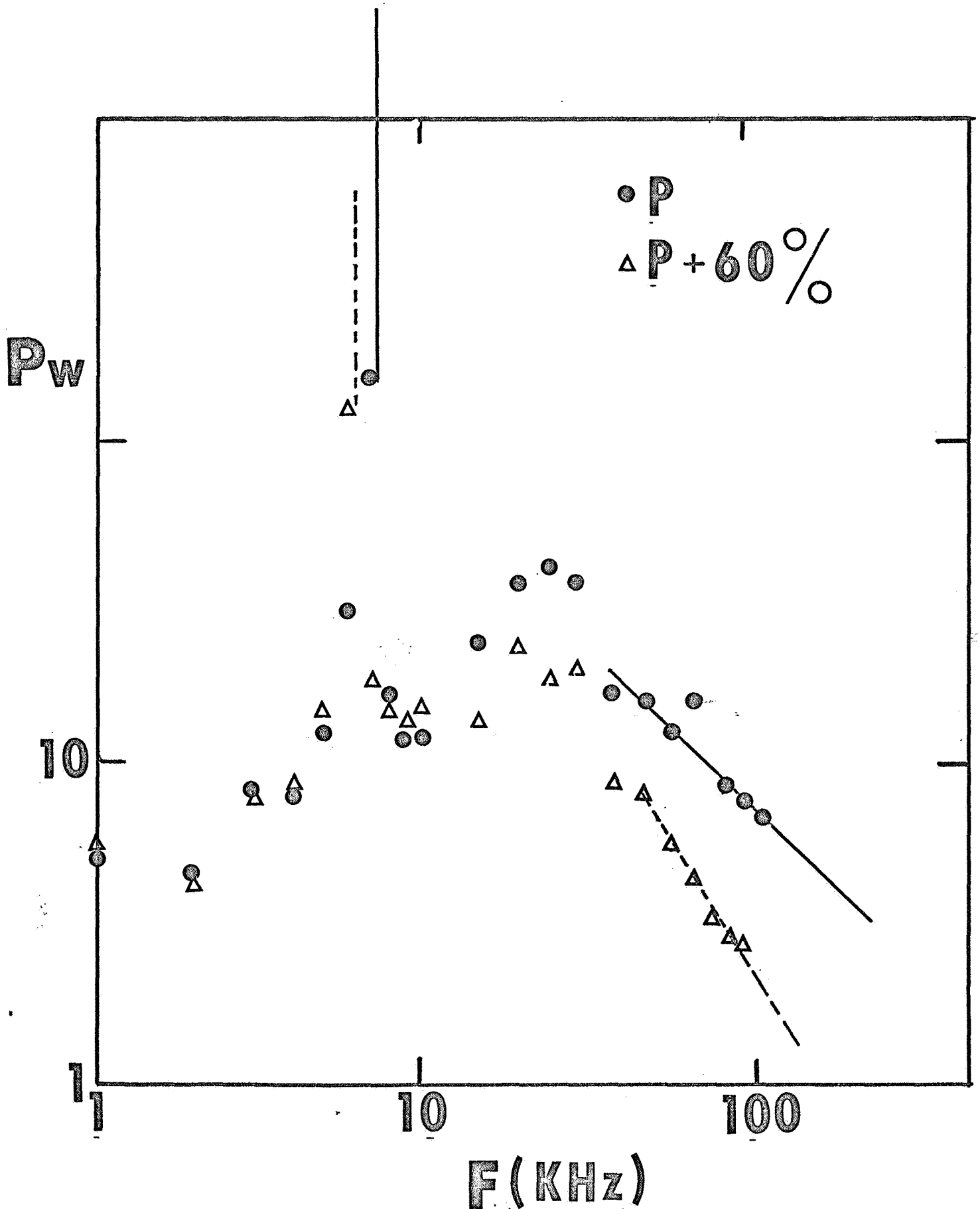


Figure 2-3 Power Versus Frequency. (drift wave) Power in arbitrary units -  
initial pressure  $P = 1.9 \times 10^{-4}$  torr,  $B_H = 2100$  gauss,  $B_C = 2100$  gauss

large coherent oscillation is present in the spectrum of oscillations, and that the type of instability determines which process is dominant.

Our results show therefore that (a) both the amplitude and the shape of the power spectrum depend on the operating conditions of the arc. (b) The shape of the power spectrum depends on whether or not an instability is present. (c) The three instabilities investigated must involve different energy exchange mechanisms. However no clear criterion is available for distinguishing between collisional and collisionless regimes in the plasma. Therefore unambiguous interpretation of our results is difficult at this stage of the investigation.

### III. Degree of Coherence in Turbulent Portion of the Spectrum

The term "coherent oscillation" in the following discussion means an oscillation which can be detected over a finite spatial region of the plasma, and is observable for a finite time. This is not a precise definition, but we use it to distinguish between those charged-particle density and electric-field fluctuations which occur completely at random in the plasma, and those in which a definite phase relation exists between systematic perturbations in these quantities, measurable over some definite time interval and some observable region of the plasma.

On a spectrum analyzer the observed Langmuir probe signals appear to represent random noise from the plasma, but our results show that some degree of coherence does exist throughout the frequency spectrum up to 100 KHz\*.

---

\*This is the upper limit for using our correlation technique with the present instrumentation.

An auto correlation function compares a signal with itself over a length of time  $\tau$ . Mathematically this is expressed as

$$C_{11}(\tau) = \lim_{T \rightarrow \infty} \frac{1}{2T} \int_{-T}^T f_1(t) f_1(t + \tau) dt \quad 3-1$$

For example the auto correlation function of wide band noise (a purely random signal with no coherence) can be seen in Figure 3-1. The magnitude of the auto correlation function at  $\tau = 0$  on the curve is a measure of the magnitude of the mean square value of the amplitude of the oscillations in the wide band noise

$$C_{11}(0) = \frac{1}{2T} \int_{-T}^T f_1^2(t) d\tau \quad 3-2$$

For times greater than  $\tau = 0$ , the auto correlation function falls to zero. This is due to the fact that signal  $f_1(t)$  is purely random, with no coherence. Therefore after  $f_1(t)$  is displaced an amount  $\tau$ ,  $f_1(t)$  and  $f_1(t + \tau)$  are no longer coherent with one another.

On the other hand the auto correlation function of a pure sinusoidal oscillation is itself a repeating sinusoid (Figure 3-2). Mathematically this can be written in the form

$$\begin{aligned} C_{11}(\tau) &= \lim_{T \rightarrow \infty} \frac{1}{2T} \int_{-T}^T \sin \omega t \sin \omega (t + \tau) dt \\ &= \lim_{T \rightarrow \infty} T \left[ \frac{1}{2T} \int_{-T}^T \sin \omega t \sin \omega t \cos \omega \tau dt \right. \\ &\quad \left. + \frac{1}{2T} \int_{-T}^T \sin \omega t \cos \omega t \sin \omega \tau dt \right] \\ &= \frac{1}{2} \cos \omega \tau \end{aligned} \quad 3-2$$

An auto correlation function taken over a wide band of frequencies from the plasma has its greatest contribution from any coherent oscillation rather than the incoherent portion of the spectrum. For example, if the spectrum of oscillations consisted of wide band noise plus one coherent oscillation at a discrete frequency  $f$ , for times later than  $\tau = 0$ ,  $C_{11}(\tau)$  would become a repeating sinusoid at the same frequency  $f$ , and for large enough  $\tau$ , the repeating sinusoid would decay as the discrete oscillation began to lose coherence with itself.

When the operating conditions of the arc are set so that no large instability at any particular frequency is present in the observed spectrum analyzer display, the auto correlation function of the resulting signal does not have the shape associated with wide band noise. Such an auto correlation function is shown in Figure 3-3. This case is intermediate between the auto correlation function computed for wide band noise and the one for a pure repeating sinusoid. A possible interpretation of the form of  $C_{11}(\tau)$  is that many short term coherent oscillations at different frequencies are superimposed on one another at the spatial location in the plasma where the probe is located. We therefore instituted a new technique of restricting the bandwidth of the incoming signal from the probe. The signal from the Langmuir probe was passed through a narrow band-pass filter, adjusted to center on the frequency  $f$  to be studied. Since the signal level was low, a low noise wide-band amplifier was then used to increase the amplitude of the transmitted signal. This signal was then fed into a variable Q selective amplifier, also centered on the frequency  $f$ , in order to obtain

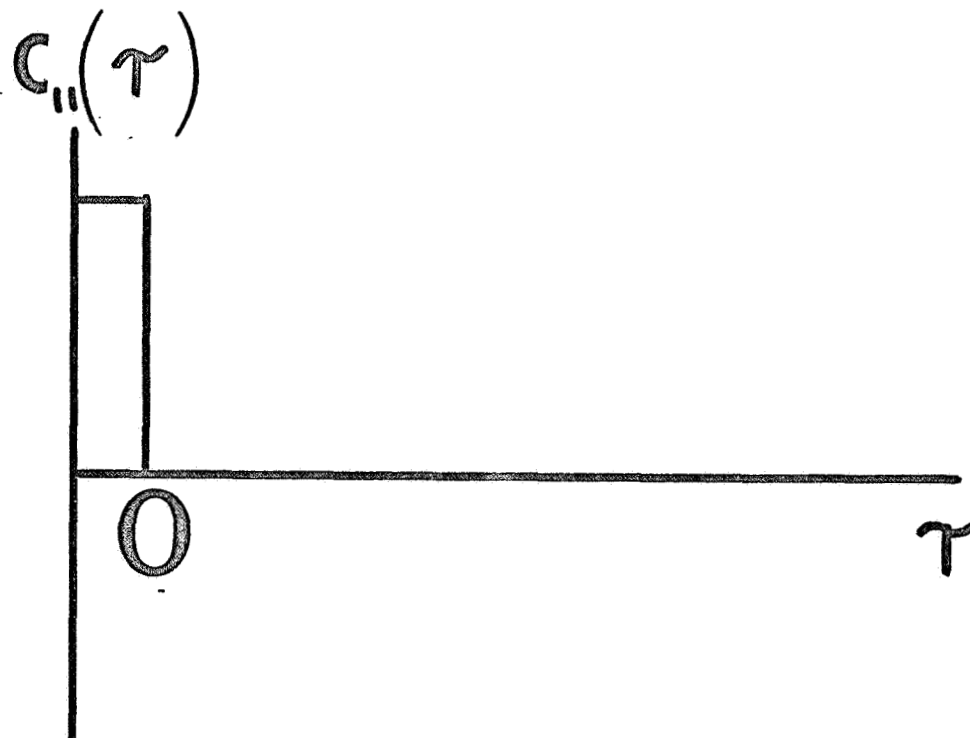


Figure 3-1 Auto correlation Function of Wide Band Noise versus  $\tau$  ( $\tau = 0$  expanded on scale).

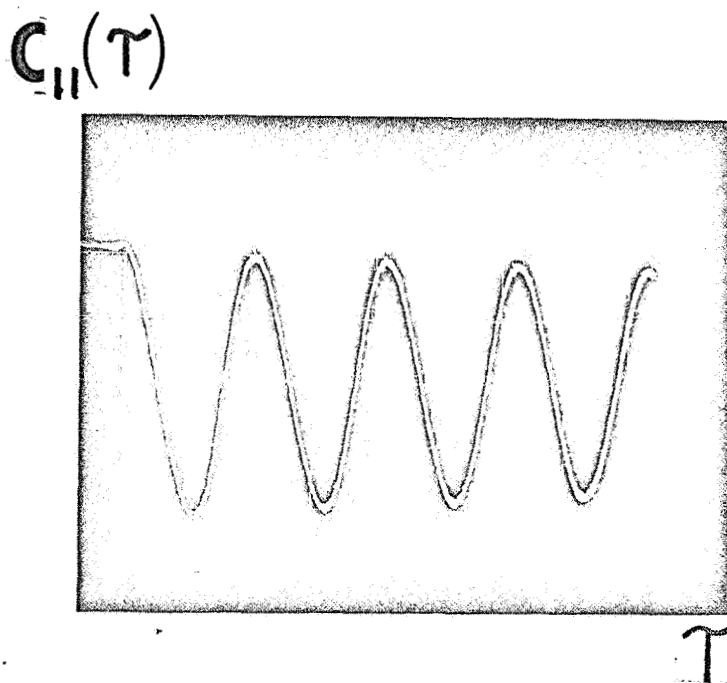


Figure 3-2 Auto correlation Function of Repeating Sinusoid versus  $\tau$



a high enough amplitude for it to be processed by the correlator. The final signal was then fed into the correlator which printed out the auto correlation function vs  $\tau$  (quasi-time) on an X-Y recorder.

We found that even when the center frequency of the filter was set on a portion of the turbulent spectrum that was considered to be totally random in nature, the resulting auto correlation function  $C_{11}(\tau)$  showed a definite sinusoidal behavior, with amplitude decaying in time. This can be seen in Figure 3-4.

We must allow for the possibility that the form of this auto correlation function could be produced by instrumentation, e.g., the response of "ringing" filters, rather than by the plasma. However there is experimental evidence which shows that the plasma does determine the observed form of the correlogram: this involves the time scales of coherence observed, and the phase shifts which are measured.

The time scale of coherence,  $\tau_c$ , is the time<sup>9</sup> it takes for an auto correlation function to decay to  $1/e$  of its value at  $\tau = 0$ . If the observed auto correlation functions were due entirely to instrumentation, their relative magnitudes might be affected by plasma conditions in the region of the probe from which the signal is derived, but the time scale for decay of the correlogram should be independent of the operating conditions of the arc. Our results clearly show that the time scales are affected by internal plasma parameters. Figure 3-5 shows a plot over one order of magnitude of time scales of coherence versus frequency, measured from the correlograms obtained over the plasma turbulence spectrum, and plotted for

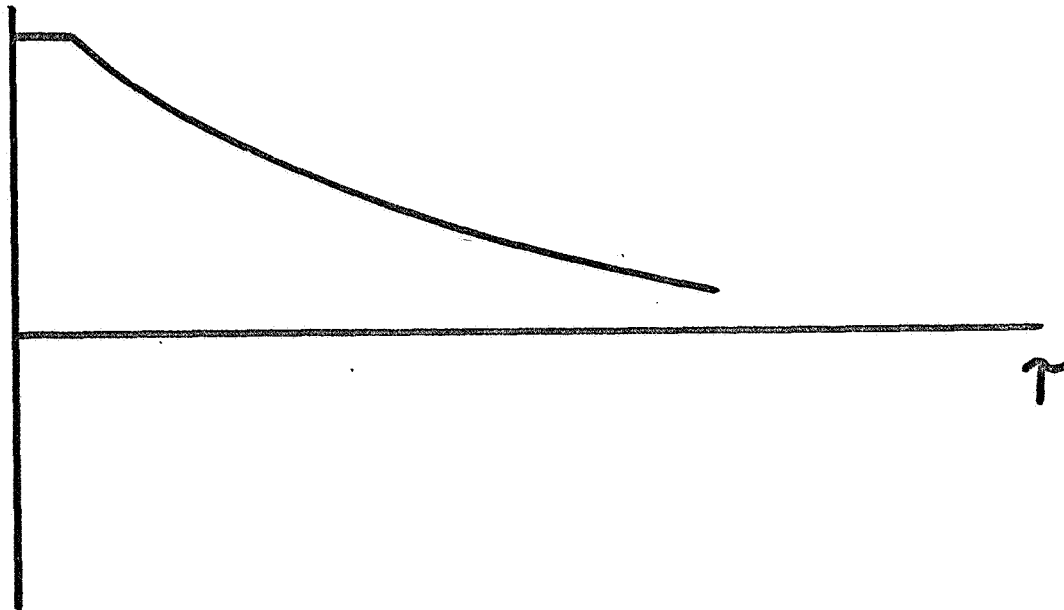
$C_{II}(\tau)$ **ALL F**

Figure 3-3 Auto correlation Function of Signal detected by a Langmuir Probe at Floating Potential placed in the Plasma. (No large instability present).

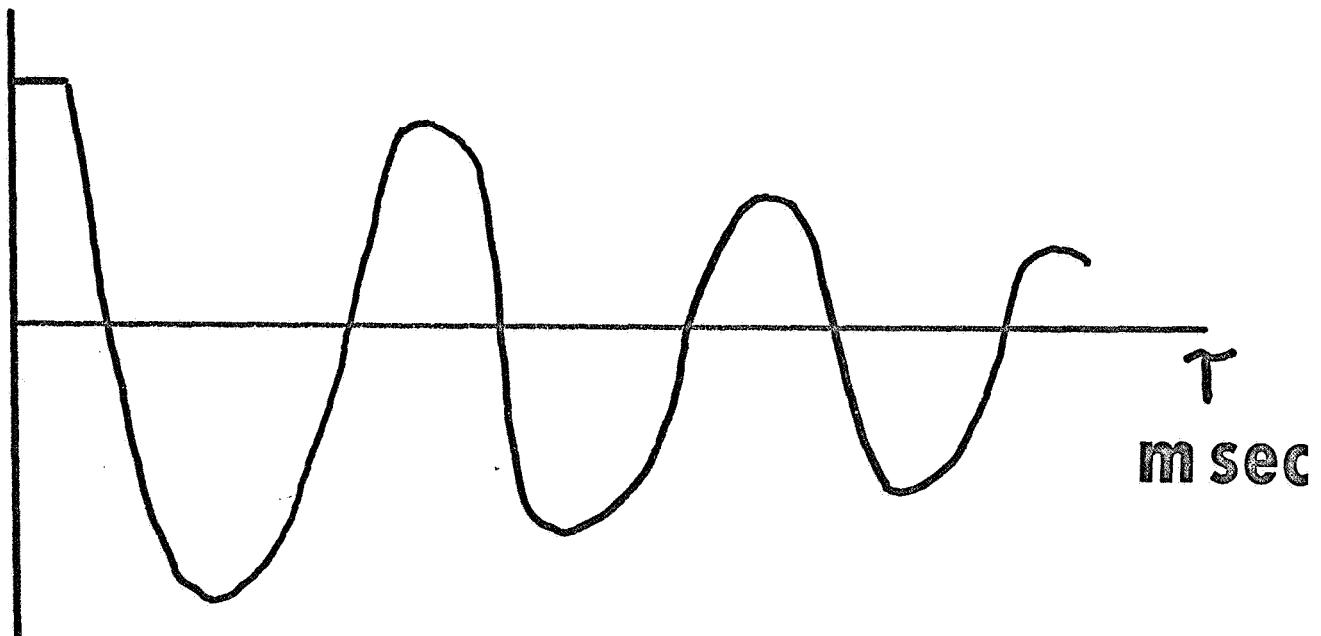
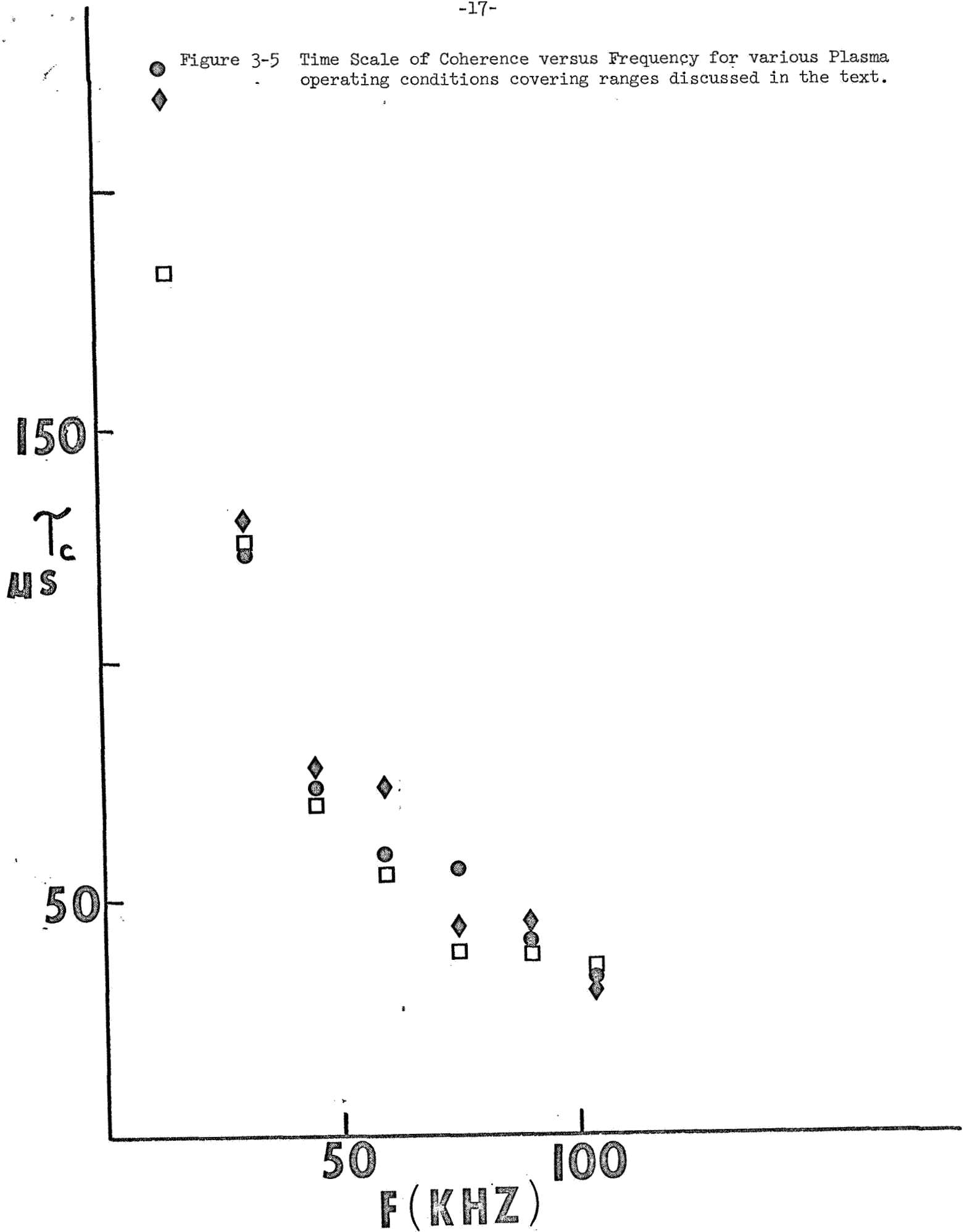
 $C_{II}(\tau)$ 

Figure 3-4 Auto correlation Function of Signal detected by a Langmuir Probe at Floating Potential placed in Plasma (Large instability present).

Figure 3-5 Time Scale of Coherence versus Frequency for various Plasma operating conditions covering ranges discussed in the text.



many different operating regions of the arc. It can be seen by comparing these points that  $\tau_c$  varies as much as 25% under different arc conditions. Even if part of the auto correlation function computed is due to the instrumentation involved, a measure of the relative change in the time scale of coherence at each frequency due to the plasma itself can be calculated from  $C_{11}(\tau)$ . We are developing a computer program to separate out the true coherence decay time scale from the correlograms in order to obtain reliable absolute values for  $\tau_c$  due to the plasma alone.

Although it is not clear whether some of the calculated decay time is associated with the process of filtering the signal, the consistent measurement of changes in phase at different spatial positions shows that the plasma is determining the form of the correlogram. This point is discussed more fully in a later section.

The length of time an oscillation remains coherent with itself is directly connected to energy dissipative mechanisms taking place in the plasma and the time scale for an oscillation to be modified or completely destroyed, shows how long energy is remaining in an oscillation at a specific frequency. We therefore investigated how the coherence time of oscillations in the turbulent portion of the frequency spectrum depended on the presence of a large instability. Figure 3-6 is a plot of coherence time of oscillations versus frequency where two separate cases are shown, one with an ion acoustic wave present in the spectrum of oscillations, the other with this instability no longer observable on the spectrum analyzer. Clearly the coherence times involved do not depend on the presence of the ion acoustic wave; there is no coupling, for example, between the ion acoustic wave at 4 KHz and the oscillations between 15 KHz and 100 KHz.

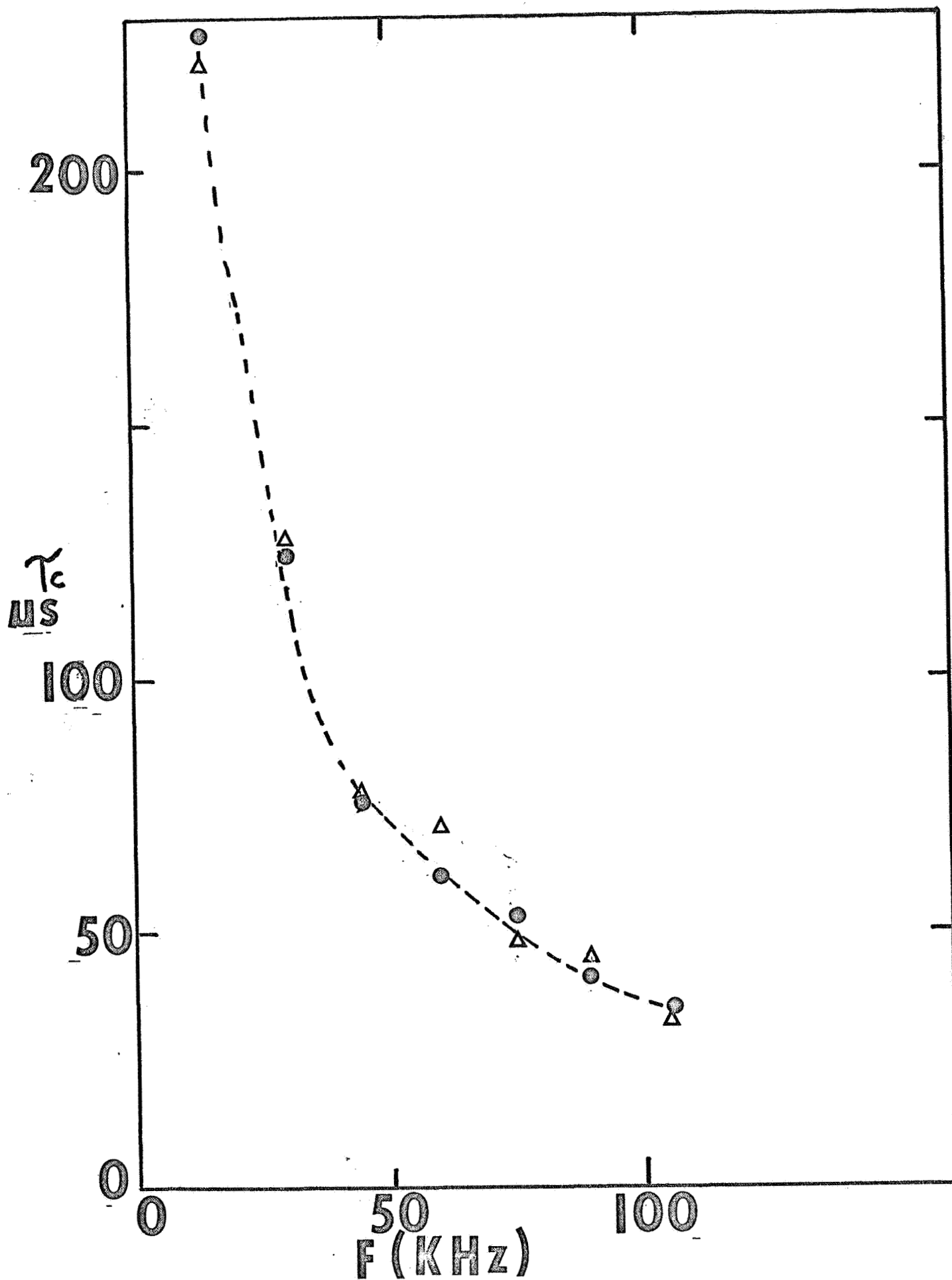


Figure 3-6 Time Scale of Coherence versus Frequency for two Plasma arc operating conditions (with and without an ion acoustic wave present)

In summary, the quantity  $\gamma_c$ , which is a measure of how long an oscillation survives, shows that (a) there is a degree of coherence in some oscillations in the frequency spectrum up to at least 100 KHz. (b) values of  $\tau_c$  over the turbulent spectrum are independent of the presence of a strongly coherent oscillation.

A further point to be considered is that when our probe is located at one position in the arc, the observed decaying auto correlation function may be due to two separate plasma effects. The first is that the oscillation is being modified as time goes by and is losing coherence with itself. The second factor affecting the apparent decay rate is convection of the oscillation past the single probe. If an oscillation in the plasma is moving past the stationary probe with some fixed velocity, with different amplitude in different regions of the plasma, any apparent changes detected by the probe will not be truly representative of the local region of the plasma in which the oscillation occurs. We need therefore to obtain a "moving-frame auto correlation function", which is a calculated auto-correlation function that simulates an auto correlation function taken from a probe moving at the convection velocity of the oscillation. In order to find the moving frame auto correlation function we have to measure cross correlation functions of a number of spatially separated probes.<sup>7</sup> This method of measuring  $\tau_c$  for an oscillation that is moving past a stationary probe is discussed in a later section. At the present time our measurements do not allow for this effect.

#### IV. Propagation Characteristics

The important propagation characteristics of plasma oscillations, such as wave number, wavelength, and speed of propagation (phase velocity), may

be determined by monitoring the cross-correlation functions of signals detected by two spatially separated Langmuir probes. The cross-correlation function is obtained by passing the detected signals into a PAR Model 100 Signal Correlator which performs electronically a close approximation to the mathematical definition:

$$C_{12}(\tau) = \lim_{T \rightarrow \infty} \frac{1}{2T} \int_{-T}^T f_1(t) f_2(t + \tau) dt \quad 4-1$$

Therefore the cross correlation function compares two separate signals over a length of time  $\tau$ . This is not the same as for the auto correlation function which compares a signal with itself.

If both  $f_1(t)$  and  $f_2(t)$  are purely random wide band noise, the resulting cross correlation function will be zero for all times since there will be no correlation between  $f_1(t)$  and  $f_2(t)$ , even at  $\tau = 0$ , because the integral

$$C_{12}(0) = \lim_{T \rightarrow \infty} \frac{1}{2T} \int_{-T}^T f_1(t) f_2(t) dt \quad 4-2$$

does not represent a mean square value of either function.

For the case of two pure repeating sinusoids of the same frequency the cross correlation function will be a repeating sinusoid. The value of  $C_{12}(\tau)$  at  $\tau = 0$  is determined by the phase relation between the two sine waves. If the two waves are represented by  $\sin(\omega t + \phi_1)$  and  $\sin(\omega t + \phi_2)$  where  $\phi_1$  and  $\phi_2$  are the phase angles involved, it can be shown that the cross correlation function

$$C_{12}(\tau) = \lim_{T \rightarrow \infty} \frac{1}{2T} \int_{-T}^T \sin(\omega t + \phi_1) \sin(\omega t + \omega\tau + \phi_2) dt \quad 4-3$$

can be written as

$$C_{12}(\tau) = (1/2) \cos \omega \tau \cos \phi + (1/2) \sin \omega \tau \sin \phi \quad 4-4$$

where  $\phi$  is the phase difference between the two sinusoids

$$\phi = \phi_2 - \phi_1 \quad 4-5$$

From 4-4 we can see that the value of  $C_{12}(\tau)$  when  $\tau = 0$  depends on the phase difference  $\phi$ ,

$$C_{12}(0) = \frac{\cos \phi}{2} \quad 4-6$$

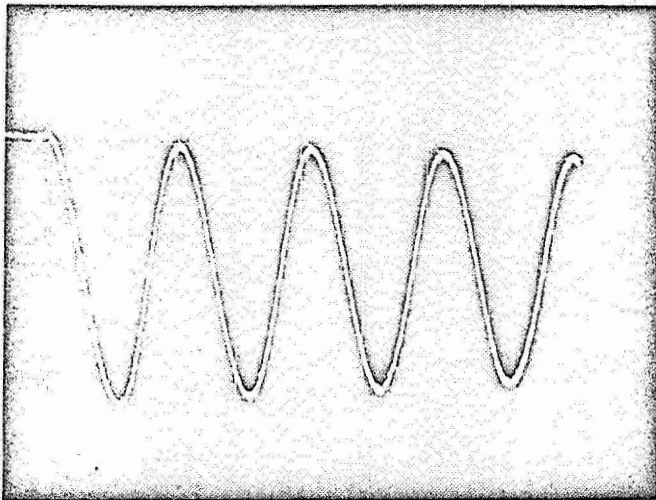
Therefore if the two sine waves are in phase, ( $\phi = \phi_2, \phi = 0$ ),  $C_{12}(0)$  will have its maximum value of 1/2 at  $\tau = 0$ . If  $\phi = \phi_2 - \phi_1 = 90^\circ$ ,  $C_{12}(0) = 0$ , and if  $\phi = 180^\circ$ ,  $C_{12}(0) = -1/2$ . Some graphical examples of this can be seen in Figure 4-1.

If the two sine waves have a different frequency the orthogonality of the sine and cosine functions causes the cross correlation function to be zero for all time  $\tau$ , since

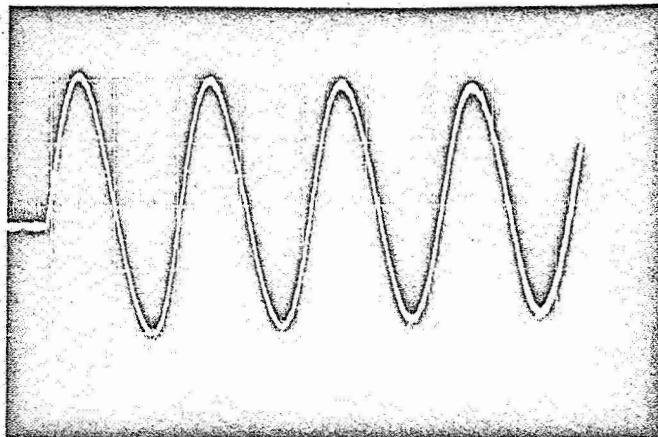
$$C_{12}(\tau) = \lim_{T \rightarrow \infty} \frac{1}{2T} \int_{-T}^T \sin \omega_1 t \sin \omega_2 (t + \tau) dt = 0, \omega_1 \neq \omega_2 \quad 4-7$$

The two spatially separated Langmuir probes in the arc pick up signals  $f_1(t)$  and  $f_2(t)$ , both of which are fed into the signal correlator. If the same oscillation is being detected at both probes, the observed form of the cross correlation function will show a sinusoidal variation with time.<sup>5,8,14,15</sup> If several different oscillations occur at both probes the resulting form of the cross correlation function will represent the superposition of the sinusoids that would result from each separate oscillation.

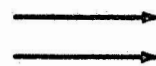




$f_1(t)$



$f_2(t)$



$C_{12}(\tau)$

-23-

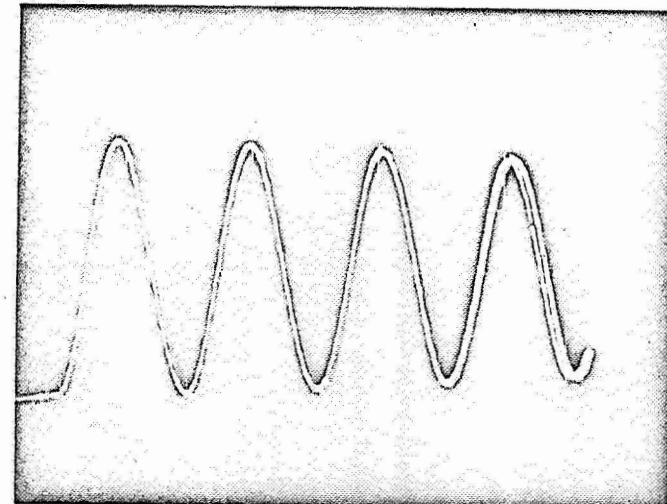
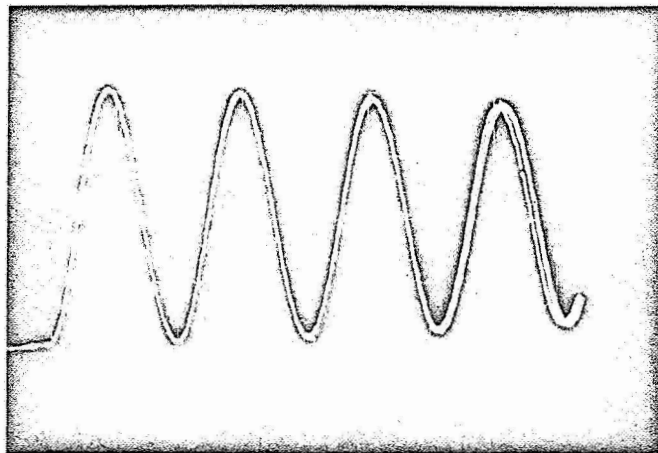
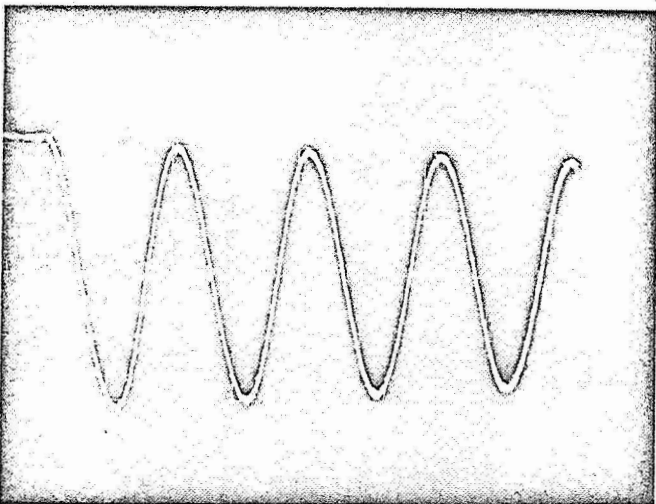


Figure 4-1 Cross correlation function of  $f_1(t)$  and  $f_2(t)$  for two separate phase differences.

Therefore a study of the cross correlation function of signals from two floating Langmuir probes gives information about properties of the electrostatic fluctuations in the plasma:

1. If the cross correlation function displays a sinusoidal variation with  $\tau$ , the signal from probe 1 contains the same oscillation as the signal from probe 2. Therefore the size or spatial extent of this oscillation must be at least the spatial separation of the probes.

2. If a sinusoidal variation with  $\tau$  is observed, the value of the cross correlation function at  $\tau = 0$  can be used to calculate the phase difference  $\phi$  in the oscillation at points 1 and 2. Further, if the spatial separation of the two probes is systematically changed, by monitoring the change in  $\phi$  one can calculate some of the propagation characteristics (wave number, wavelength, speed of propagation) of the oscillation.

An illustration of the change in  $\phi$  with changing probe separation is given in Figure 4-2 for the case of a coherent instability of large amplitude<sup>8</sup>. Four different correlograms are shown, taken using two radially movable probes placed in the arc in a region of the plasma where a strong ion acoustic wave was observed on the spectrum analyzer. When these probes were aligned with one another (curve No. 1) the resulting correlogram had its maximum value at  $\tau = 0$  where the phase of the ion acoustic wave at both probes is approximately the same. Curves 2-4 shows that as one probe was moved radially away from the other probe (3 steps of 1/2 cm displacement each) the value of  $C_{12}(\tau)$  at  $\tau = 0$  is no longer a maximum. The maximum in the correlogram has shifted to the right as the probes are separated. This shows that the ion acoustic wave is propagating in the

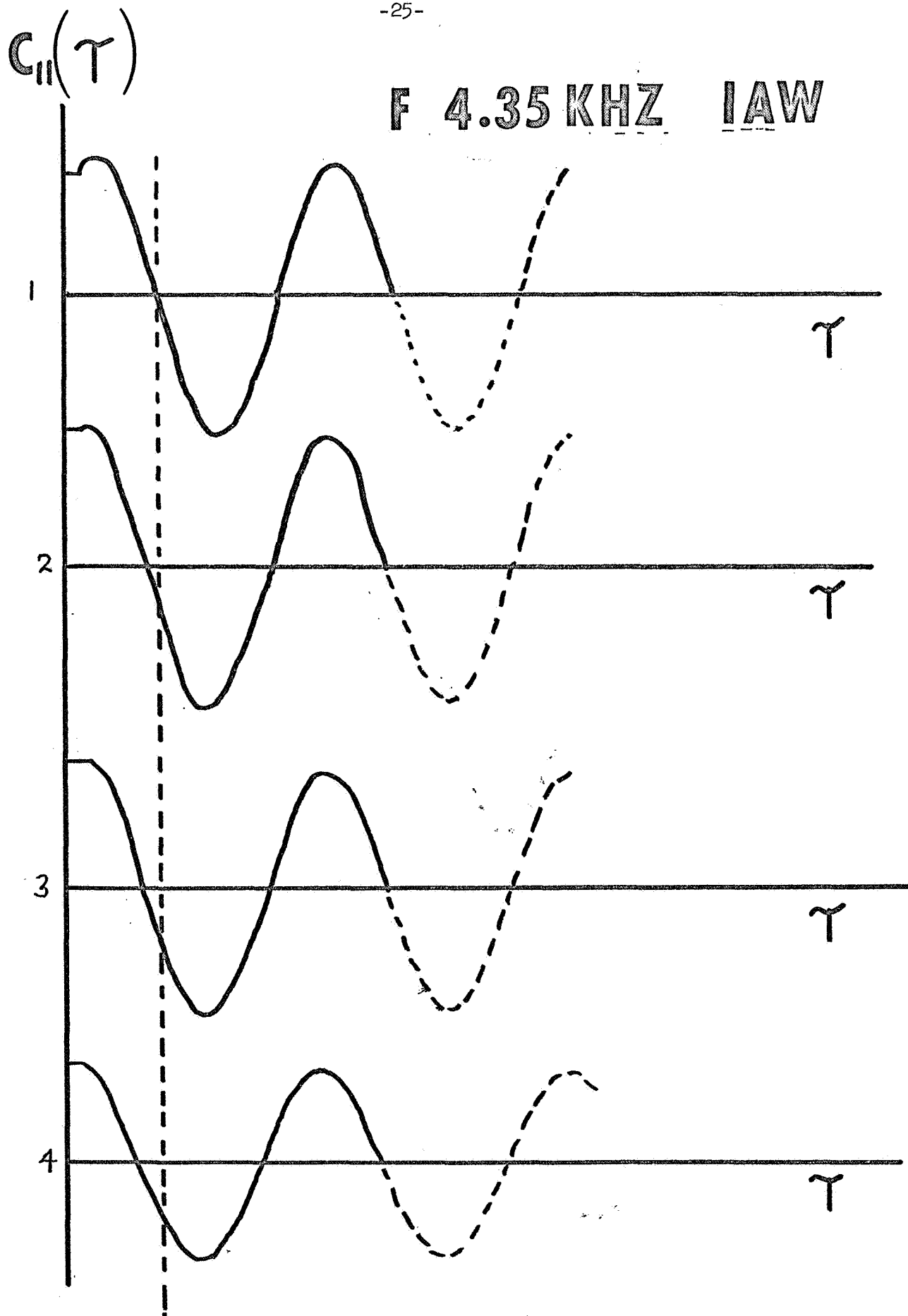


Figure 4-2 Cross correlograms for four different probe separations.

radial direction. Determination of its phase velocity from measurement of radial phase shifts show a radial phase velocity of approximately  $7.4 \times 10^4$  cm/sec.

The phase shift,  $\Delta \phi$ , with changing probe separation was measured by observing the first zero crossing of successive correlograms. From eqn. 4-4 at the point  $\tau_1$ , where the first zero crossing occurs

$$C_{12}(\tau_1) = 0 = 1/2 \cos \omega \tau_1 \cos \phi + 1/2 \sin \omega \tau_1 \sin \phi \quad 4-8$$

As the probe separation changes, the point at which the first zero crossing occurs at  $\tau_2 \neq \tau_1$ . The corresponding quantity which must also change in equation 4-8 is the phase difference  $\phi$ . A simple graphical technique for determining the shift of the first zero crossing from  $\tau_1$  to  $\tau_2$  was used to calculate  $\Delta \phi$ .

In order to see whether or not the same oscillation occurs at two spatially separated points in the plasma and to be able to calculate the phase difference,  $\phi$ , of this oscillation at these two points, only one correlogram is necessary (see eqn. 4-4). But if one wants to monitor a phase shift,  $\Delta \phi$ , with changing probe separation as indicated above, several correlograms are needed. The phase shift  $\Delta \phi$  can thus be used to calculate propagation characteristics of the oscillation. Assuming the relationship

$$\phi = kl \quad 4-9$$

where  $k$  is the wave number of the oscillation, and  $l$  is the separation of the probes corresponding to a phase difference  $\phi$ , the wave number  $k$  can be

directly calculated from the measured value of  $\phi$ . Note that three separate measurements are required for full information, since  $k_r$ ,  $k_z$  and  $k_\phi$  must be determined independently.

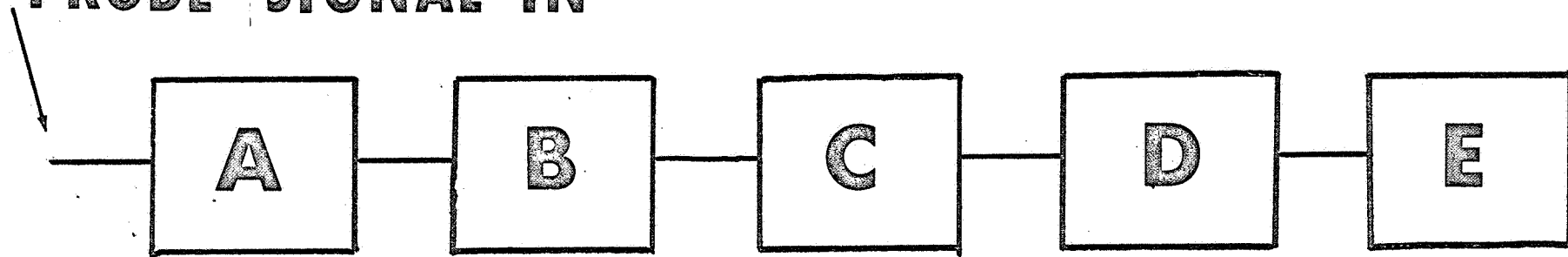
If we know the wave number for separate frequencies in the spectrum ( $\omega = \omega(k)$ ) we can plot the dispersion relation for the plasma point by point. From this curve both the phase velocity and the group velocity can be calculated

$$v_p = \omega/k ; \quad v_g = d\omega/dk \quad 4-10$$

In order to investigate the propagation characteristics of oscillation at selected frequency intervals throughout the turbulent portion of the frequency spectrum, the signals from each of the two probes was fed through separate identical filter and amplifier circuits (see Fig. 4-3). Just as for the case of the ion acoustic wave, when the radial separation between two probes is altered, the correlograms showed a phase shift,  $\Delta\phi$ .

In figure 4-4, which involves an oscillation at 15 KHz, as one probe is moved in relation to the other, the time  $\tau$  at which the maximum value of  $C_{12}(\tau)$  occurs changes, and the first zero crossing of  $C_{12}(\tau)$  shifts to the right. This indicates a phase shift  $\Delta\phi$  from which  $k_r$ , and  $v_p$  for this oscillation can be calculated. It was found that  $\Delta\phi = 48^\circ$  for 1/2 cm displacement  $k_r = 1.18 \text{ cm}^{-1}$ ,  $\lambda_r = 3.74 \text{ cm}$  and  $v_p = 5.6 \times 10^4 \text{ cm/sec}$ . A similar set of curves can be seen in figure 4-5 for an oscillation at 60 KHz. In this case a 1/4 cm displacement led to a  $50^\circ$  phase shift  $k_r = 3.4 \text{ cm}^{-1}$ ,  $\lambda_r = 1.8 \text{ cm}$  and  $v_p = 1.08 \times 10^4 \text{ cm/sec}$ . Therefore for the ion acoustic wave at 4 KHz, and the oscillations at 15 KHz and 60 KHz our preliminary measurements show that in the radial direction the phase velocity decreases with increasing frequency of the oscillation.

**PROBE SIGNAL IN**



**A - FILTER**

**D - CORRELATOR**

**B - AMP**

**C - FILTER**

**E - X Y REC.**

Figure 4-3 Filter A -  $Q = 0.4$ , Amplifier B PAR Model 213 low noise wide band, Filter C PAR Model 210 selective amplifier  $Q = 10$ , Correlator D - PAR Model 100 signal correlator.

$$F = 15 \text{ KHz}$$

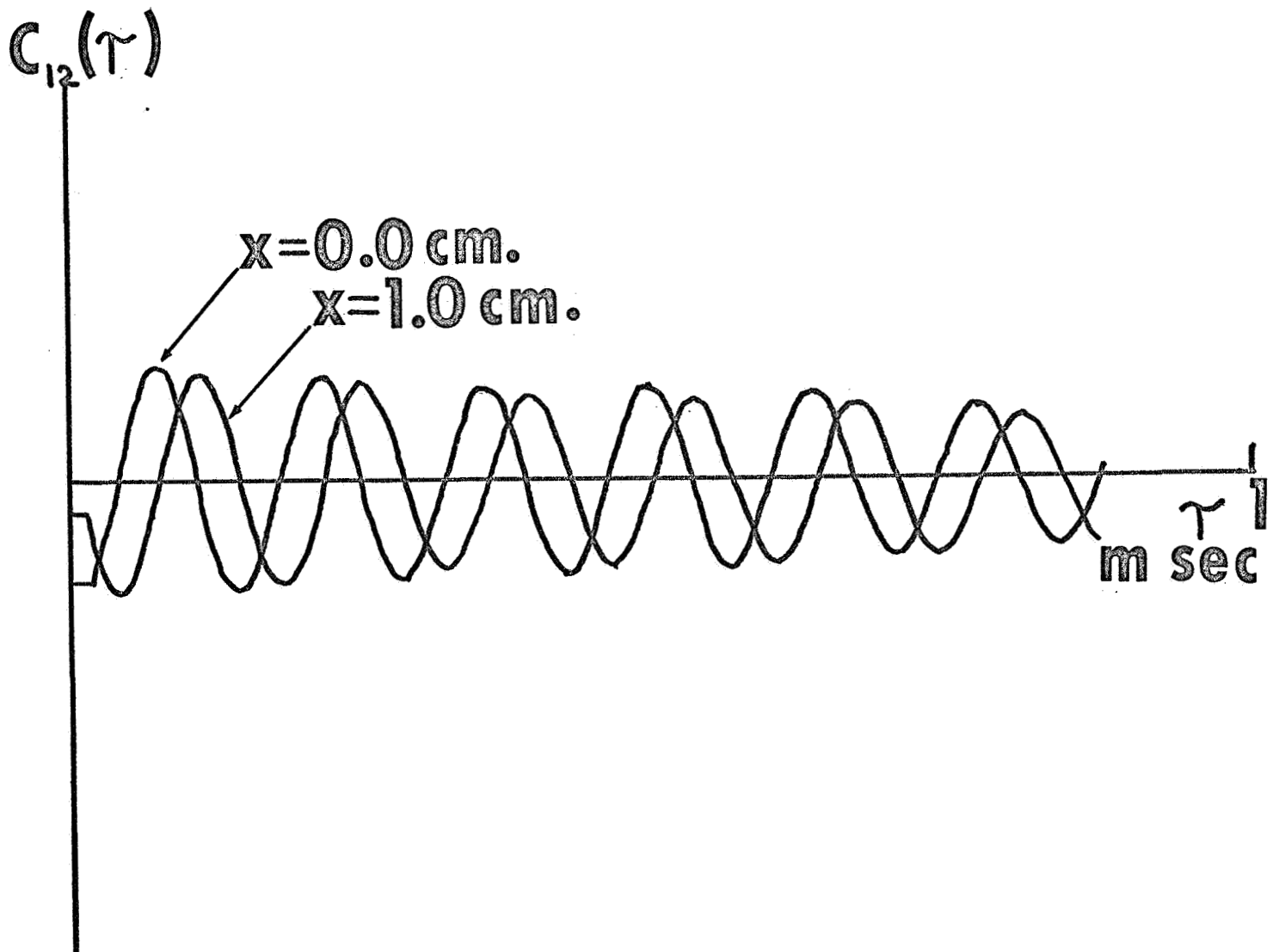


Figure 4-4 Cross correlograms for two different probe separation; frequency of oscillation = 15 KHz.

$$F = 60 \text{ KHz}$$

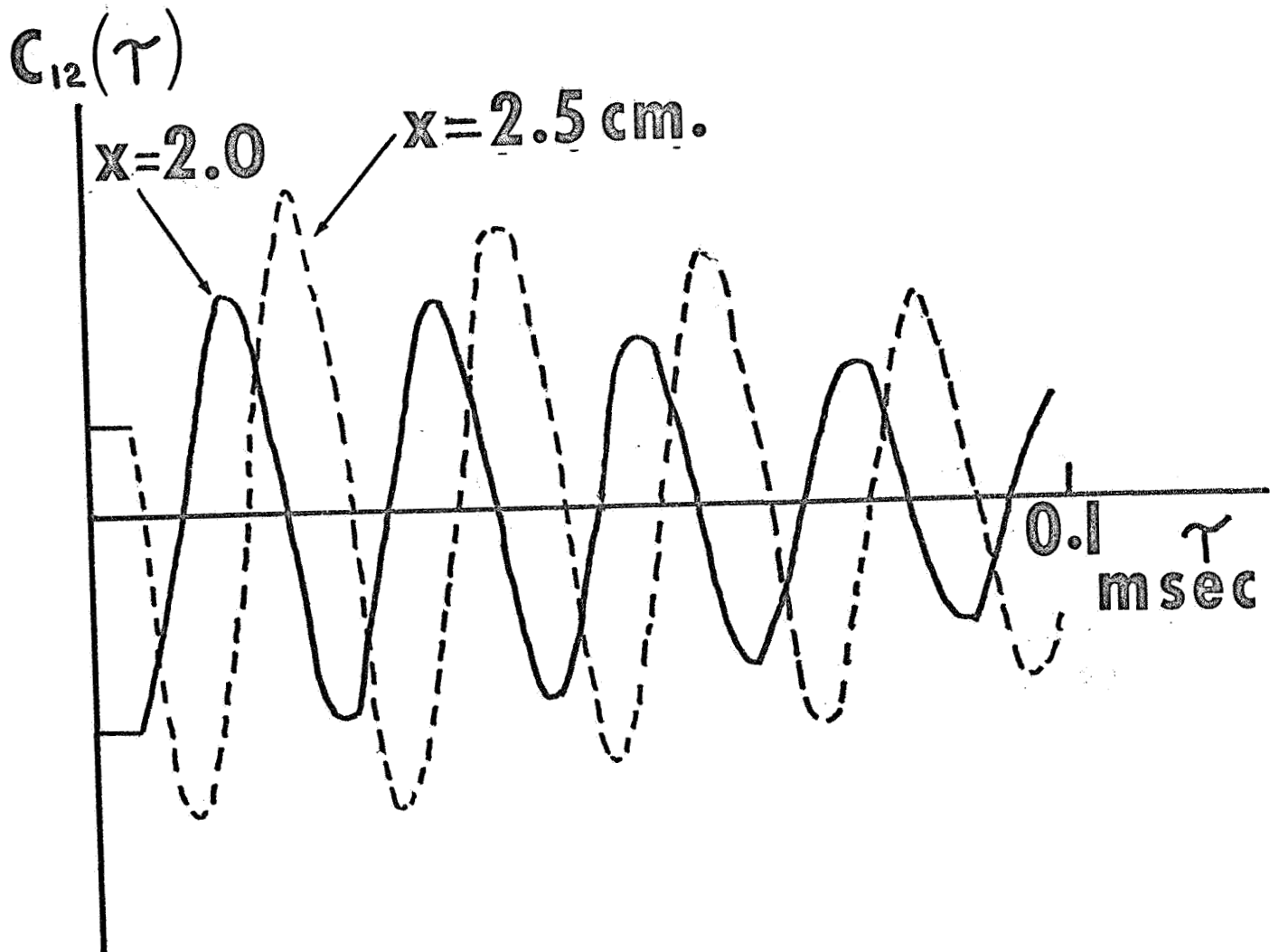


Figure 4-5 Cross correlograms for two probe separations; frequency of oscillation = 60 KHz.



Preliminary measurements have shown that consistent changes in the phase shift  $\Delta \phi$  with radial separation only occur over small radial lengths. Therefore the calculated values for  $k_r$  depend on the radial positions at which the two probes have been placed. We interpret this as showing that only small radial sections or layers of the plasma can be considered homogeneous enough to yield interpretable results. Because of this, the dispersion relation  $\omega = \omega(k)$  is definitely not a simple relationship.

#### V. Frozen and Non-Frozen Flow

Care must be taken when interpreting correlation measurements in the presence of appreciable turbulence intensity. Shear forces, for example, may be continually creating and modifying the turbulence. In this case Taylor's hypothesis that turbulence may be regarded as a frozen pattern of eddies moving past an observer, is no longer valid. It has been shown for the case of fluid turbulence that Taylor's frozen flow hypothesis is valid only if the level of turbulence is low, viscous forces are negligible, and the mean shear is small<sup>11</sup>. If one cannot assume a frozen flow, interpretation of correlation measurements become more difficult.

For the case of frozen flow at some convection velocity, a signal registered by a stationary probe at one point will be identical with that registered further "downstream" at a second position  $x_1$  but will occur at a time  $\tau_1$  later. The cross correlation function  $C_{12}(\tau)$  will be a maximum at  $\tau = \tau_1$  and the velocity of convection,  $U_c$ , of the pattern may be defined as  $x_1/\tau_1$ .

The cross correlation function can be written as

$$C_{12}(\tau_1) = C_{12}(x = U_c \tau_1) \quad 5-1$$

If a number of cross-correlation measurements are performed at separations of  $x_i$  ( $i = 1, 2, 3, \dots$ ), each curve will pass through its maximum value when  $\tau = \tau_i = x_i/U_c$ . The auto-correlation in a frame of reference which is moving with the convection velocity will be a straight line, always equal to a constant, namely the maximum value of the cross correlation function. The Weiner Auto-Correlation Theorem will lead to a power spectrum in which all the power can be found in an infinitely narrow band of frequencies centered at zero frequency. If the observer were to remain stationary, the spectrum observed would be due to eddies moving past at the convection velocity and not due to any temporal turbulence fluctuations<sup>7</sup>.

Any fixed-frame frequency  $f$  is related to the spatial extent,  $\lambda$ , of the eddy producing the observed signal, by a relation of the form

$$f = U_c/\lambda \quad 5-2$$

or

$$\omega = 2\pi f = kU_c \quad 5-3$$

where  $k$  is the wave number of the eddy. Therefore the convection velocity, spatial extent, and wave number of eddies in a frozen flow may be determined from a knowledge of the spectrum of oscillations and a series of cross-correlation measurements.

For the case of a non-frozen flow a series of cross-correlation curves will still rise to a maximum at some value of  $\tau$ , but this maximum value

will now be a function of  $x$ , the separation. This is because the flow is now being modified as it moves downstream. The convection velocity can no longer be defined by the time delay at which the maximum of a particular measuring point separation. If an observer were to move at the convection velocity while measuring the auto correlation function,  $C_{11}(\tau)$  would be the envelope of the cross correlation curves. The convection velocity would be defined by the time delay at which this envelope of all the cross correlation curves intersects the curve for a particular measuring point separation (see Fig. 5-1).<sup>7</sup>

If an observer were stationary the auto correlation function he would measure would have two effects associated with it. 1) The eddy is being modified 2) the eddy is being swept past. When discussing a time scale of coherence, only the modification of turbulence with time should be taken into account. Therefore for both the frozen and non-frozen pattern of turbulence the time scale of coherence as discussed in an earlier section, should be derived from a moving frame auto correlation. Note that in the frozen flow situation this auto correlation function will lead to a  $\tau_c$  which is infinite, since the definition of a frozen flow is that the pattern of turbulence is not changing with time.

We have not yet determined under what conditions the plasma oscillations can be considered to be in a frozen or non-frozen flow. Until this determination is made the time scale of coherence has some ambiguity associated with it, because our measured values include both the modification of the turbulence and the effect of the oscillations moving past the measuring point. It should be noted here that if the convection of the

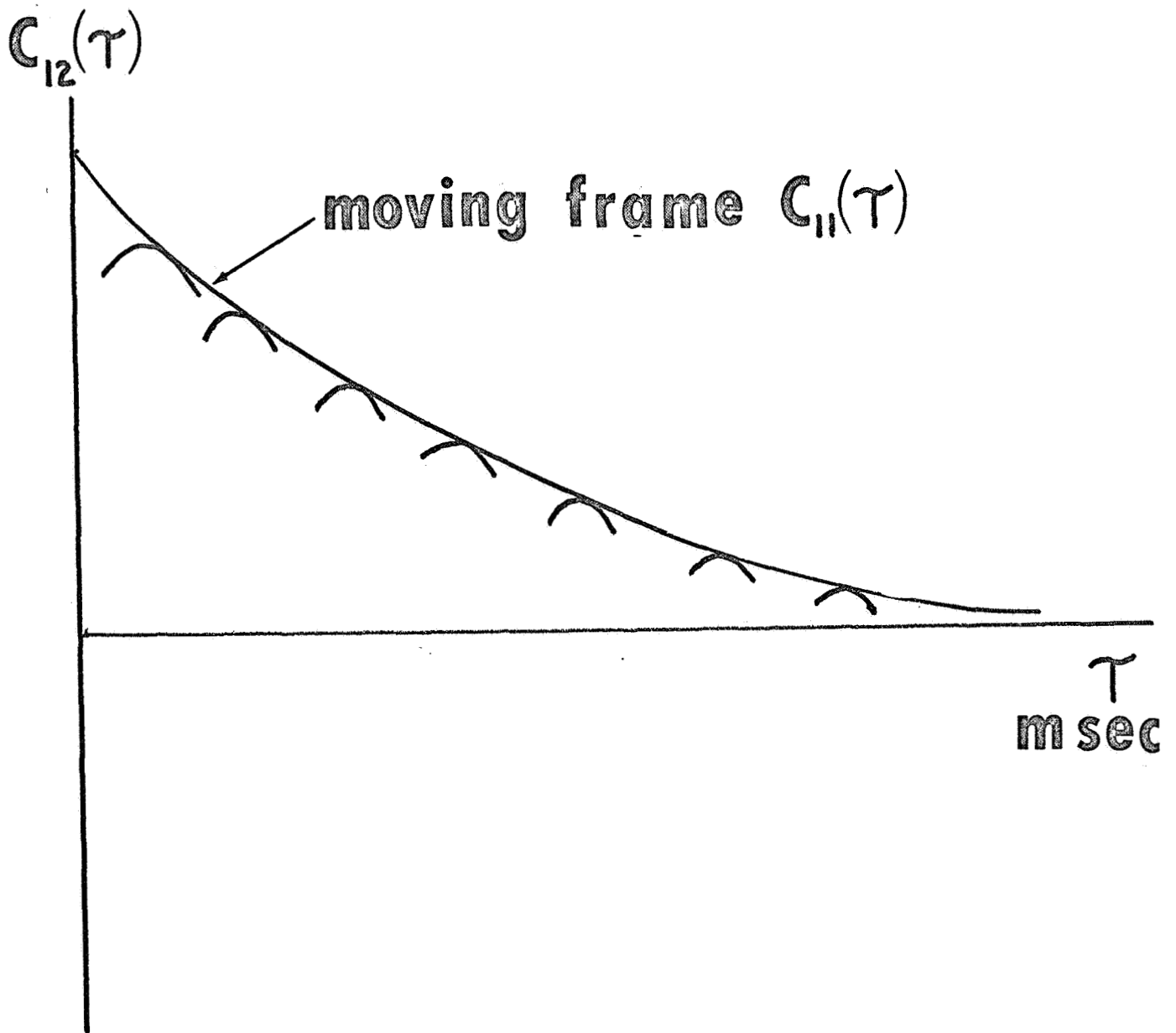


Figure 5-1 Cross correlation function maximum versus  $\tau$  for increasing probe separation (probe separation increasing left to right).

oscillations past the probe is slow in comparison to the time it takes for an oscillation to be significantly modified, the time scales of coherence quoted will be very close to the true value.

The measurements necessary to decide whether or not the plasma flow is frozen or continually being created and destroyed and those measurements needed to determine the convection velocity of the oscillation are being carried out at the present time.

## VI. Length Scales of Coherence and Strength of Turbulence

The concept of a time scale of coherence was defined as a quantity which leads to an order of magnitude estimate of how long an oscillation remains in a specific form. Another quantity of interest is the length scale of coherence which determines over what spatial extent of the fluid the eddy or oscillation retains the same general form before it is significantly modified.

The length scale of coherence,  $l_c$ , is defined in much the same way as the time scale except the definition of  $l_c$  utilizes the cross correlation function. The length scale of coherence is defined as the length over which  $C_{12}(\tau, x)$  at  $\tau = 0$  drops to  $1/e$  of its maximum value<sup>9</sup>. Preliminary measurements taken in the radial direction have shown that  $l_c$  varies as much as an order of magnitude in the frequency range 15 KHz - 100 KHz.

$\tau_c$  and  $l_c$  are quantities which involve the spatial and temporal extent of the turbulent oscillations. In order to completely describe the turbulent behavior of the plasma one needs a quantity which will indicate the strength or level of turbulence. The ratio of the a.c. fluctuation in charged particle

density  $n'$  to the measured d.c. charged particle density  $n_0$  is one such quantity. In our hollow cathode discharge  $n'/n_0$  varies from 0.1% up to 10%, depending upon the externally set operating conditions of the arc.

Another term used in discussion of hydrodynamic turbulence is the "intensity of turbulence", which is defined as the ratio of the rms velocity of the flow to the mean velocity<sup>10</sup>.

$$\frac{u'}{u} = 1/3 \left[ \frac{U}{l_c} \tau_c \left( \frac{U l_c}{\nu} \right)^{1/2} \right]^{-2/3} \quad 6-1$$

where  $\tau_c$  and  $l_c$  are the time and length scales of coherence respectively and  $\nu$  is the kinetic viscosity of the plasma. This quantity describes the plasma turbulent phenomena in terms of fluid turbulence terminology, time scale of coherence, power spectrum, length scale of coherence and an intensity of turbulence. Discussion of our results therefore requires consideration of the above parameters, and also whether we are dealing with collisional or collisionless plasma for comparison with theoretical predictions. Clarification of these points requires further work.

#### Reports and Publications

Dr. Noon reported on the progress of the work at NASA Lewis Center, Cleveland, in April 1970. A paper has been prepared for the November meeting of the Plasma Physics Division of the American Physical Society: "Correlation Measurements of Plasma Turbulence Spectra", G. Huchital, J. H. Noon, and W. C. Jennings.

#### Acknowledgment

Active discussions with Dr. K. Thom, the technical monitor for this research program, are gratefully acknowledged.

References

1. Buchel'nikova, Salimov and Eidelman, "Plasma Turbulence in the Presence of a Drift Instability, JETP 24, 548, 1967.
2. Buchel'nikova, Salimov and Eidelman, "Excitation of an Ion-Acoustic Instability in an Inhomogeneous Plasma", Sov. Phy. Tech. Phy. 12, 1072, 1968.
3. Buchel'nikova, Salimov and Eidelman, "Investigation of Plasma Turbulence Due to the Ion Acoustic Instability", JETP, 25, 252, 1967.
4. Chen, F. F., Spectrum of Low-B Plasma Turbulence, Phy. Rev. Let. 15, 381, 1965.
5. Chung, K. and Rose, D. J., "Correlation Study of a Drift Wave Instability", App. Phy. Let. 11, 247, 1967.
6. Eastlund, Josephy, Leheny and Marshall, "Wave-Excited Anomalous Diffusion in a Fully Ionized Magnetoplasma", Phy. of Fluids, 7, 12, Dec. 1966.
7. Fisher and Davis, "Correlation Measurements in a Non-Frozen Pattern of Turbulence", Jour. Fluid Mech. 18, 97, 1964.
8. Gunshor, R. L., J. H. Noon, and E. H. Holt, "Correlation Measurements of Ion Acoustic Waves in a Highly Ionized Plasma", Phys. Fluids 11, 1796 (1968).
9. Guthart, Weissman and Moritz, "Measurement of the Charged Particles of an Equilibrium Turbulent Plasma", Phys. Fluids, 2, 1766, 1966.
10. Hinze, Turbulence, McGraw Hill, 1960.
11. Lin, C. C., "On Taylor's Hypothesis and the Acceleration Terms in the Navier-Stokes Equations", Quant. App. Mech. 4, 295, 1953.
12. J. H. Noon, H. A. Schmidt and E. H. Holt, "Connection between Self Excited Low Frequency Oscillations and Anomalous Plasma Diffusion", Plasma Phys. 12, 477 (1970).
13. Porkolab and Kino, "Turbulent Diffusion Experiment in a Thermal Plasma", Phys. Fluids, 11, 346, 1968.
14. Serafini, J. S., "Correlation Measurements of Plasma Fluctuations in a Hall Current Acceleration", NASA-TMX - 52366.
15. Serafini, J. S., "On the Utility of Conventional Turbulence Experimental Methods in the Study of Plasma Fluctuations", NASA A68-17866.

16. Tchen, C. M., "Turbulent Diffusion of a Plasma Across a Magnetic Field", Proceedings of the Symposium on Turbulence of Fluids and Plasmas, New York 1968, Polytechnic Press.
17. Tchen, C. M., "Spectrum and Diffusion in a Turbulent Plasma with Collisional and Collisionless Dissipations", Proceedings of the Symposium on Turbulence of Fluids and Plasmas, New York 1968, Polytechnic Press.
18. Thomassen, K. I., "Turbulent Diffusion in a Penning-Type Discharge", Phy. Fluids 9, 1836, 1966.